J. Membrane Biol. 200, 67–81 (2004)
DOI: 10.1007/s00232-004-0694-7

The Journal of
Membrane
Biology

Intracellular Delivery of Carbohydrates into Mammalian Cells through Swelling-activated Pathways

R. Reuss[1], J. Ludwig[1], R. Shirakashi[2], F. Ehrhart[1], H. Zimmermann[3], S. Schneider[4], M.M. Weber[5], U. Zimmermann[1], H. Schneider[1], V.L. Sukhorukov[1]

[1]Lehrstuhl für Biotechnologie, Biozentrum, Universität Würzburg, Am Hubland, 97074 Würzburg, Germany
[2]Institute of Industrial Science, The University of Tokyo, 4-6-1 Komaba Meguro-ku, 153-8505, Tokyo, Japan
[3]Abteilung Kryobiophysik & Kryotechnologie, Fraunhofer-Institut für Biomedizinische Technik, 66386 St. Ingbert, Germany
[4]Allgemeine Innere Medizin, Endokrinologie und, Diabetologie, Universitätsklinik Bochum, 44789 Bochum, Germany
[5]Schwerpunkt für Endokrinologie and Stoffwechselerkrankungen, I. Medizinische Klinik und Poliklinik, Universitäts-Klinik Mainz, 55131 Mainz, Germany

Received: 1 March 2004/Revised: 21 June 2004

Abstract. Volume changes of human T-lymphocytes (Jurkat line) exposed to hypotonic carbohydrate-substituted solutions of different composition and osmolality were studied by videomicroscopy. In 200 mOsm media the cells first swelled within 1–2 min and then underwent regulatory volume decrease (RVD) to their original isotonic volume within 10–15 min. RVD also occurred in strongly hypotonic 100 mOsm solutions of di- and trisaccharides (trehalose, sucrose, raffinose). In contrast to oligosaccharide media, 100 mOsm solutions of monomeric carbohydrates (glucose, galactose, inositol and sorbitol) inhibited RVD. The complex volumetric data were analyzed with a membrane transport model that allowed the estimation of the hydraulic conductivity and volume-dependent solute permeabilities. We found that under slightly hypotonic stress (200 mOsm) the cell membrane was impermeable to all carbohydrates studied here. Upon osmolality decrease to 100 mOsm, the membrane permeability to monomeric carbohydrates increased dramatically (apparently due to channel activation caused by extensive cell swelling), whereas oligosaccharide permeability remained very poor. The size-selectivity of the swelling-activated sugar permeation was confirmed by direct chromatographic measurements of intracellular sugars. The results of this study are of interest for biotechnology, where sugars and related compounds are increasingly being used as potential cryo- and lyoprotective agents for preservation of rare and valuable mammalian cells and tissues.

Key words: Cell volumetry — Regulatory volume decrease — Osmotic stress — Trehalose — Inositol — Sorbitol — Jurkat cells — T-lymphocytes — Volume-sensitive channels

Introduction

Various sugars, sugar alcohols and other carbohydrates are found at high concentrations in organisms that are capable of withstanding extreme environmental conditions, including freezing, desiccation and hypersalinity. The disaccharides trehalose and sucrose accumulate in anhydrobiotic and cold-tolerant yeasts, plants and some animals (e.g., tardigrades, nematodes) [5, 40, 53]. The monosaccharide glucose provides cryoprotection to wood frogs [43]. Other mono- and oligosaccharides, such as galactose, maltose, lactose and raffinose, as well as sugar alcohols, alone or in various combinations, have also been reported to protect cells and seeds against dehydration and cold [4, 25, 33]. In addition, a wide range of cells respond to chronic hypersalinity with elevated cytosolic levels of sugar alcohols, most notably inositol and sorbitol, which exert stabilizing effects on cellular proteins and membranes [19, 22, 38, 44]. Based on their ability to induce cryo- and lyotolerance, sugars and sugar alcohols have found a variety of biomedical applications. These include stabilization of frozen and/or dry macromolecules (e.g., antibodies, enzymes, chromatin, etc. [39]), preservation of artificial and

Correspondence to: U. Zimmermann; email: zimmermann@biozentrum.uni-wuerzburg.de

natural membranes, as well as whole cells and organs [2, 8, 13].

Several experimental techniques have been explored to introduce non-native sugars, such as trehalose, sucrose, etc., into mammalian cells to confer desiccation or cold tolerance. These techniques include the expression of genes for trehalose synthesis [13], microinjection of trehalose and other oligosaccharides into oocytes [9], trehalose uptake by cells during the membrane phase transition or via the fluid-phase endocytosis [2, 36, 52]. In a different approach, a pore-forming protein from a genetically engineered *Staphylococcus aureus* has been inserted into the membrane of mammalian cells to allow the introduction of exogenous trehalose [8]. Electroinjection can also be used for intracellular trehalose delivery [41]. High cytosolic concentrations of some sugars and sugar alcohols (inositol, sorbitol) have been achieved in mammalian cell lines by long-term (days) cultivation in hyperosmotic media [21, 44]. Despite their efficiency, most techniques for intracellular sugar delivery (except electroinjection) are restricted to a specific cell type (e.g., microinjection into large oocytes) or they are unacceptable for medical applications (e.g., gene/protein manipulations).

The present study addresses native membrane transport mechanisms, particularly those involved in the regulation of cell volume, as possible pathways for the introduction of exogenous saccharides into mammalian cells. Volume regulation is a basic property of various animal cell types and tissues. Even under continuous hypotonic stress imposed by decreased external osmolality, most cells can re-adjust their normal isotonic volume after transient osmotic swelling by a mechanism known as regulatory volume decrease (RVD). During RVD, the initial cell swelling induces coactivation of volume-sensitive Cl^- and K^+ channels, thus leading to the net efflux of KCl, osmotically inevitable water loss and to the restoration of normal cell volume. The fundamentals of cell volume regulation in mammalian cells have been described in detail elsewhere [10, 26, 28, 32, 34, 45].

Numerous biophysical and biochemical studies have demonstrated that some volume-sensitive anion channels not only allow the passage of small inorganic anions (e.g. Cl^- efflux during RVD), but are permeable for large organic anions, zwitterionic and neutral osmolytes, including amino acids, sugars and sugar alcohols [7, 19, 20, 23]. Swelling-activated release of organic solutes (e.g., inositol, sorbitol, etc.) has been reported from a very wide range of mammalian cells [22, 46]. These findings suggest that exposure of cells to hypotonic sugar-substituted solutions, in which the concentration gradient favors sugar entry into the cells, may mediate substantial uptake of certain sugars by cells through swelling-activated channels. Consequently, activation of these dormant transport pathways may well be a useful approach for the introduction of non-native carbohydrates as potential cryo- and lyoprotectants into mammalian cells.

In this study, we explored the volume response of human T-lymphocytes (Jurkat line) to an acute hypotonic challenge in media of different sugar composition. We found that RVD took place in strongly hypotonic solutions (100 mOsm) containing an oligosaccharide (trehalose, sucrose or raffinose) as the major osmolyte. In contrast, partial or even no RVD occurred in strongly hypotonic solutions of monosaccharides (glucose, galactose) or monomeric sugar alcohols (inositol, sorbitol). Theoretical analysis of the volumetric data using a simple phenomenological RVD model suggested the presence of volume-sensitive pathways in the cell membrane conducting selectively monomeric sugars and polyols but being poorly permeable for oligosaccharides. Chromatographic determination of intracellular sugar contents confirmed the selective uptake of monomeric carbohydrates by hypotonically stressed Jurkat cells.

Materials and Methods

Cells

All experiments were performed on Jurkat cells, a human leukemic cell line, obtained from the American Type Culture Collection (ATCC, Manasses, Virginia, USA). Cells were cultured in complete growth medium (CGM) containing RPMI 1640 supplemented with 10% fetal calf serum, 2 mM L-glutamine, 100 U/ml penicillin, 100 μg/ml streptomycin, 2 mM sodium-pyruvate, 1 × MEM non-essential aminoacids (PAA, Linz, Austria) and 50 μM 2-mercaptoethanol (Sigma, Deisenhofen, Germany), at 37°C under 5% CO_2. Every day, the cell cultures were diluted 3:7 with CGM to keep the cells in the log phase.

Hypotonic Solutions and Chemicals

All sugars and sugar alcohols of highest purified grade, including glucose (*glu*), galactose (*gal*), trehalose (*tre*), sucrose (*suc*), raffinose (*raf*), inositol (*ino*) and sorbitol (*sor*), as well as the channel blockers 5-nitro-2(3-phenyl-propylamino) benzoic acid (NPPB) and 4,4′-diisothiocyanatostilbene-2,2′-disulfonic acid (DIDS) were purchased from Sigma or Fluka (both Deisenhofen, Germany). In RVD experiments, hypotonic solutions of osmolalities 100 and 200 mOsm (mosmol/kg) were used, which contained, respectively, 90 and 190 mM carbohydrate as well as about 5 mM HEPES-KOH (pH 7.2). The osmolality of solutions was determined cryoscopically (Osmomat 030, Gonotec GmbH, Berlin, Germany).

Cell Volumetry

Cell volume changes were measured in a 50-μl flow chamber designed for rapid exchange of media. The transparent body and floor of the chamber were made of PMMA (plexiglass) and a 0.15-mm thick glass coverslip, respectively. To enhance cell adhesion,

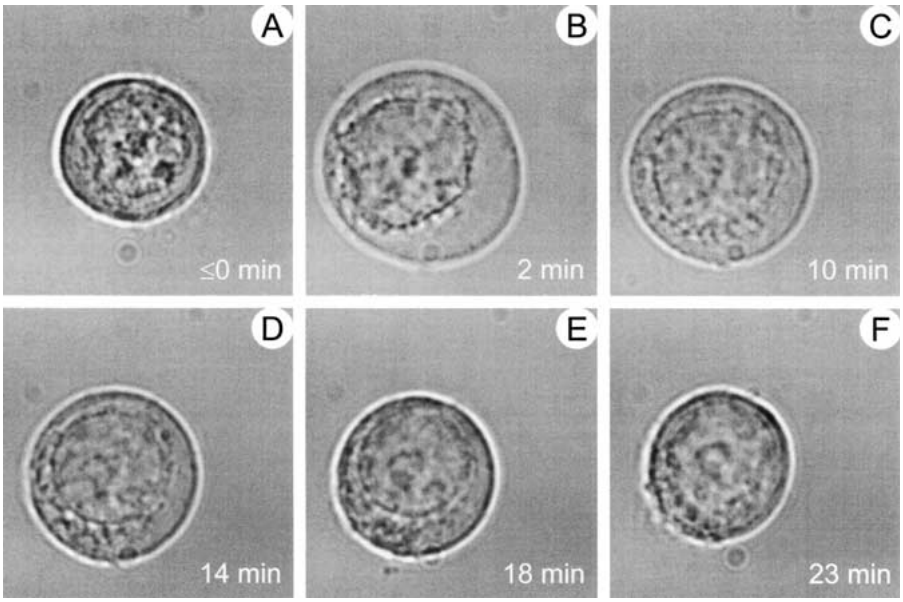

Fig. 1. Fast swelling and regulatory volume decrease (RVD) of a Jurkat cell in 100 mOsm medium containing 90 mOsm trehalose and 10 mOsm electrolyte. The microphotographs show the same cell before (*A*, isotonic CGM) and after acute hypotonic challenge (B–F) at the indicated time intervals. In isotonic CGM (*A*, time $\leq$ 0), the cell had a radius r of 9.4 μm, corresponding to the original isotonic volume $V_0 \approx 3.5$ pL. Upon medium replacement at zero time, the cell swelled to $V_{max} \approx 8.4$ pL ($r \approx 12.6$ μm) within 2 min (*B*) and then shrank gradually to its isotonic size within 10–23 min (*C–F*).

the coverslip was pretreated for 5–10 min at room temperature with 0.5 mg/ml poly-D-lysine (Sigma) [37, 51]. At a flow rate of about 1 ml/min the exchange of solutions in the chamber took about 2 s from the moment of turning the tap.

Before videomicroscopic measurements, an aliquot of cells suspended in isotonic CGM (300 mOsm) at a density of about 10^5 cells/ml was injected into the flow chamber and the cells were allowed to settle and to adhere to the glass coverslip for 10–15 min. The chamber was placed on the stage of a microscope (BX50, Olympus, Hamburg, Germany) and the cells were viewed with a 40 × objective in transmitted light. The microscope was equipped with a CCD video camera (SSC-M370CE, Sony, Cologne, Germany) connected to the video digitizing board of a personal computer [48]. Images of cells were taken 1 min before and at various time intervals (20–60 s) up to 25 min after medium exchange, using WinTLV software (C3 Systems, UK). The cross-section areas (A) of 3–9 cells per microscopic field were determined with an image analysis program (ScionImage; Scion, Frederick, MD). At each time interval, the volume (V) of an individual cell (Fig. 1) was evaluated from its cross-section by assuming spherical geometry. The cell volume was normalized to the original isotonic volume (V_0) as: $v = V/V_0$. The mean v values (± SE) for a given experiment were calculated from a sequence of about 30 images and plotted against time after the change from isotonic (300 mOsm) to hypotonic solution (200 or 100 mOsm). Experiments for each sugar solution were performed on 2–3 separate cell passages.

Volumetric Data Analysis

The volumetric data obtained in different hypotonic sugar solutions were analyzed with a membrane transport model given in the Appendix. The model assumes the presence of volume-sensitive channels (VSC) for sugars and electrolytes in the cell membrane and allows the complex volumetric response of cells (including cell swelling and RVD) to be explained in terms of the membrane hydraulic conductivity L_p, and the volume-dependent permeabilities of sugar P_s and electrolyte P_e.

Because of the complex volume dependence of the plasma membrane permeability (Eq. A4), the system of differential equations A1–A3 cannot be solved analytically. Therefore, a numeric nonlinear regression (NNLR) procedure was devised in F77-Fortran that allowed the estimation of the unknown transport parameters L_p, P_e and P_s by fitting the VSC-model (i.e., combination of Eqs. A1–A4) to the experimental volumetric data.

Chromatography

Concentrations of sugars and sugar alcohols in cell lysates were determined using high performance anion-exchange chromatography (HPAEC) and pulsed amperometric detection (PAD). Measurements were performed on a BioLC/DX-600 IC chromatograph distributed by Dionex (Idstein, Germany). The system consisted of a gradient pump GP50 and an electrochemical detector ED50 including a detection cell with a gold working electrode and a pH-Ag/AgCl reference electrode. HPAEC CarboPac MA1 (4 × 250 mm) and CarboPac MA1 Guard (4 × 50 mm) were used as analytical and guard columns, respectively. The eluent (612 mM NaOH) was degassed with helium. The eluent flow rate was 0.4 ml/min. Sample loop and injection volumes were 25 and 100 μl, respectively. Amperometric detection settings were 0.05 V (0.40 s), 0.75 V (0.20 s), and −0.15 V (0.40 s). The acquisition and processing of chromatograms were performed on a personal computer equipped with the Dionex Peak-Net 6.0 software. Prior to sugar determinations in cell samples, the PAD peaks in the elution profiles were identified and the chromatograph was calibrated using standard sugar solutions (inositol, sorbitol, trehalose, etc.).

Preparation of Cells for Chromatographic Sugar Analysis

Aliquots of Jurkat cells (1.5×10^7 cells) were incubated for 25 min in hypotonic solutions (100 mOsm, 5 ml) containing 90 mM trehalose, inositol or sorbitol as the major osmolyte. Control cells were incubated in diluted PBS of the same osmolality. Following hypotonic treatment, each cell sample was washed twice with isotonic PBS (centrifugation at 200 × g and removal of the supernatant). An aliquot of the pellet (5 μl) was resuspended in 10 ml PBS. Cell volume and density were analyzed by electronic cell counting using a Coulter-like device (Casy, Schärfe System GmbH, Reutlingen, Germany). The remaining pellet (~45 μl) was transferred

into 1 ml deionized water and then subjected to two freeze-thaw cycles (cooling to −80°C and warming to room temperature), in order to solubilize the cells. The cell lysate was then deproteinized by incubation with 10% acetonitrile (15 min at 4°C) and centrifuged at 3000 × *g* for 15 min at 4°C. The supernatant was collected and analyzed by HPAEC-PAD. It should be noted that the trehalose content detected in cell lysates fell steadily with increasing number of washing cycles (*data not shown*). However, rigorous washing (i.e., 3–4 centrifugation/resuspension cycles) was impractical because of significant losses of viable cells available for chromatographic determinations.

Cell Viability and Proliferation

The short-term viability of hypotonically treated cells was analyzed by means of propidium iodide (PI) exclusion assay. Cells (10^5 cells/ml) were incubated in a 100 mOsm sugar-substituted solution (*glu*, *gal*, *sor*, or *ino*) for 25 min. Thereafter, 40 μM PI (Sigma) were added to the cell samples and fluorescent cell staining was measured by means of a flow cytometer (Epics XL system; Beckman Coulter, Fullerton, CA) equipped with a 488 nm argon laser. Red fluorescence (RF) signals from at least 5000 cells were detected using the band pass filter 675 ± 15 nm. The output Log RF data are presented as one-dimensional histograms, from which the percentage of viable cells is evaluated as described elsewhere [31].

To analyze the effect of hypotonic stress on the long-term viability of lymphocytes, cell proliferation and growth in culture were assessed by direct cell counting. After a hypotonic shock (25 min, 100 mOsm *glu*, *gal*, *sor*, or *ino*), cells were resuspended in CGM in 24-well multiplates at a final cell density of 5×10^4 cells/ml and then cultured for 10 days under standard conditions (*see* above). Cell density was measured immediately and at various time intervals after hypotonic shock (12, 24, 36, ... h) by means of electronic cell counting (*see* above). To estimate the initial growth rate, cell growth curves (i.e., cell density N vs time t) were fitted to the Gompertz equation [3]: $N = N_0 \exp\{\alpha/\beta[1\text{-}\exp(-\beta t)]\}$, where N_0 is the initial cell density and α/β is the initial growth rate.

Results

The magnitude and time course of cell volume changes were studied by rapid transfer of the Jurkat cells from an isotonic saline solution (300 mOsm) to a hypotonic environment. The hypotonic solutions contained one of the following sugars or sugar alcohols (polyols) as the major osmolyte: glucose, galactose, sorbitol, inositol, trehalose, sucrose and raffinose. For each sugar, the solution osmolality was adjusted to 200 and 100 mOsm.

Fast Initial Swelling

In response to hypotonicity, Jurkat cells swelled within the first 1–2 min from their original isotonic volume V_0 to the maximum volume V_{max} (Fig. 2). At the same osmolality, the relative magnitudes of initial swelling, defined as $v_{max} = V_{max}/V_0$, were similar in the presence of all sugars and sugar alcohols studied here (Table 1). At 100 and 200 mOsm, the v_{max} ranges were 1.5–1.9 and 1.2–1.3, respectively. The latter result is in good agreement with the v_{max} value of 1.18 ± 0.04 reported for this cell line (when exposed to 197 mOsm saline medium) in the literature [6].

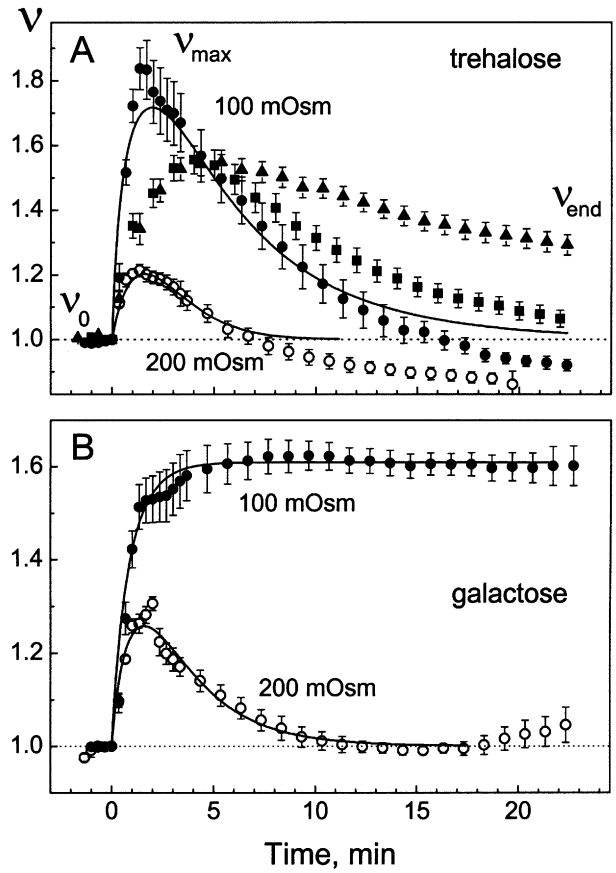

Fig. 2. Changes of the relative volume ($v = V/V_0$) of Jurkat cells in hypotonic trehalose (*A*) and galactose solutions (*B*). The cell samples were originally ($t < 0$) exposed to an isotonic saline solution (CGM). At zero time CGM was replaced by a hypotonic sugar solution. After fast initial swelling, the cells underwent RVD in slightly hypotonic solutions of both sugars (200 mOsm, *empty symbols*), as well as in strongly hypotonic trehalose medium (100 mOsm, *filled circles* in *A*). In contrast, 100 mOsm galactose completely inhibited RVD in Jurkat cells (*B*, *filled circles*). The continuous curves are the best fits of the VSC model to the data (*see* below). The anion channel blockers NPPB (100 μM) and DIDS (1 mM) inhibited RVD in Jurkat cells exposed to 100 mOsm trehalose (*A*, *filled triangles* and *squares*, respectively).

In trehalose solutions (Fig. 2*A*), the time intervals T_{max} required to reach the maximum cell volume v_{max} were 90 ± 5 and 70 ± 6 s at 100 and 200 mOsm, respectively. Similar initial swelling kinetics were observed in hypotonic galactose solutions (Fig. 2*B*). The v_{max} and T_{max} values for all sugars and sugar alcohols are summarized in Table 1.

Osmotically Inactive Volume

To estimate the osmotically inactive volume fraction in Jurkat cells, volumetric measurements were per-

Table 1. Effects of osmolality and carbohydrate composition on the initial swelling kinetics (v_{max} and T_{max}) and the secondary volume response (v_{end}) of Jurkat cells to hypotonic stress

Carbohydrate	Osmolality mosmol/kg	v_{max}[1]	T_{max}[1] s	v_{end}[2]	RVD
Galactose	200	1.31 ± 0.02	120	0.99 ± 0.01	+
	100	1.54 ± 0.05	140 ± 11	1.60 ± 0.04	–
Glucose	200	1.22 ± 0.01	80 ± 4	0.83 + 0.02	+
	100	1.67 ± 0.07	120 ± 9	1.68 ± 0.05	–
Sorbitol	200	1.27 ± 0.02	80 ± 4	0.91 ± 0.02	+
	100	1.84 ± 0.06	140 ± 3	1.95 ± 0.05	–
Inositol	200	1.15 ± 0.01	60	0.88 ± 0.03	+
	100	1.88 ± 0.06	130 ± 4	1.35 ± 0.05	partial RVD
Trehalose	200	1.21 ± 0.02	70 ± 6	0.88 ± 0.04	+
	100	1.84 ±0.08	90 ± 5	0.92 ± 0.02	+
Sucrose	100	1.67 ± 0.07	120 ± 5	0.85 ± 0.03	+
Raffinose	100	1.65 ± 0.05	130 ± 5	0.92 ± 0.04	+

[1] v_{max} and T_{max} are the mean values (± SE) of the relative magnitude of the initial cell swelling and the time interval required to reach the v_{max} volume.
[2] v_{end} is the final relative cell volume measured 20–25 min after hypotonic shock.

formed over a wide osmolality range from 100 to 500 mOsm. In contrast to hypotonic solutions (generally used in this study), the hypertonic 500 mOsm medium caused rapid transient decrease of the cell volume to its minimum value v_{min}. Afterwards the cells swelled back to their original isotonic volume within 20–25 min (*data not shown*). The experimental v_{max} and v_{min} values were plotted against the reciprocal normalized osmolality (symbols in Fig. 3) and fitted by the Boyle van't Hoff equation:

$$v_{max} = \frac{C_{iso}}{C}(1 - v_b) + v_b \qquad (1)$$

where C is the solution osmolality, the isotonic osmolality is C_{iso} = 300 mOsm, the term $v_b = V_b/V_0$ represents the osmotically inactive volume fraction at 300 mOsm. Judging by the correlation coefficient (r = 0.98), the initial osmoregulation response of Jurkat cells during the water phase is well described by the linear Boyle van't Hoff relationship. From the best least-square fit of Eq. 1 to the volumetric data obtained in inositol solutions (*filled circles* in Fig. 3), the osmotically inactive fraction was found to be v_b = 0.48 ± 0.05. The v_{max} data for other carbohydrates (*empty symbols* in Fig. 3 and Table 1) indicate that the initial swelling behavior was very similar in hypotonic solutions of different sugar alcohols, mono- and disaccharides used in this study. The osmotically inactive volume obtained here for proliferating Jurkat cells was significantly larger than those reported for quiescent human blood lymphocytes (v_b = 0.32) [12] and murine T-lymphocytes ($v_b \approx 0.28$) [29].

In a previous study [47], we found that three murine cell lines, including fibroblasts, myeloma and hybridoma cells, exhibited strongly non-linear dependences of volume on reciprocal osmolality. It should be noted, however, that volume changes in the murine cells were determined 15–40 min after exposure to hypotonic inositol, whereas the linear Boyle van't Hoff plot for Jurkat cells (Fig. 3) is

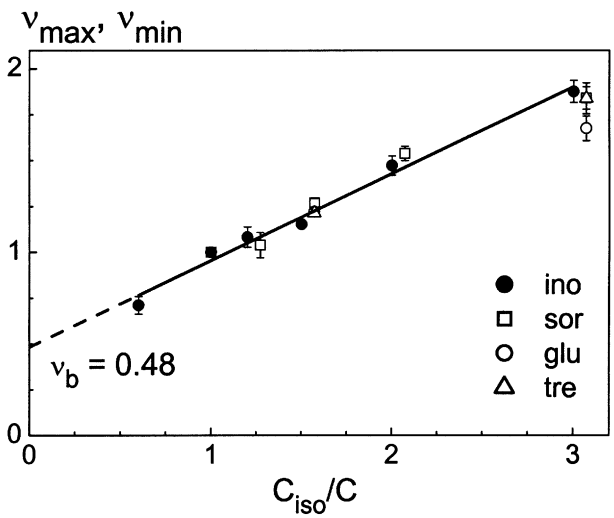

Fig. 3. Boyle van't Hoff plot for Jurkat cells in various sugar solutions including inositol (*filled circles*), sorbitol, glucose and trehalose (*empty squares*, *circles* and *triangles*, respectively). Each data point represents the mean (± SE) of normalized volume magnitudes (v_{max} or v_{min} for a 500 mOsm solution) plotted against the reciprocal normalized osmolality (C_{iso}/C, where C_{iso} = 300 mOsm) for 6–10 cells. The line shows the best least-square fit of Eq. 1 to the data obtained in inositol media (*filled circles*). From the Y-intercept, the osmotically inactive volume fraction (v_b) was found to be 0.48 ± 0.05.

based on the initial swelling magnitude data v_{max} measured 1–2 min after hypotonic shock. The departure from the linear osmometric behavior reported earlier for murine cells [47] was most likely due to the secondary volume regulation processes, such as partial RVD observed here in inositol media (*see* Table 1).

Influence of Osmolality and Sugar Composition on RVD

We found that under mild hypotonic stress, both short- and long-term volumetric responses of Jurkat cells were very similar for the different sugars (Fig. 2*AB*, *empty symbols*). After the fast initial swelling phase, the cells slowly underwent regulatory volume decrease (RVD) in 200 mOsm solutions of all carbohydrates used here (Table 1). Despite persisting hypotonicity, the cells shrank gradually and recovered their original isotonic volume (V_0) within 5–10 min. After reaching the original value, the cell volume continued to reduce modestly and stabilized at or slightly below V_0 in most sugar solutions. At 200 mOsm, the long-term v values (v_{end}) measured after 20–25 min incubation varied between 0.83 (glucose) and 0.99 (galactose, *see* Table 1). The ability of Jurkat cells to undergo RVD in 200 mOsm saline solutions has been reported earlier [6].

The use of strongly hypotonic media (100 mOsm) revealed a dramatic difference between oligosaccharides (trehalose, sucrose and raffinose) and monomeric carbohydrates (galactose, glucose, sorbitol, inositol) in their effects on the secondary (long-term) volume changes in Jurkat cells. As shown in Fig. 2*A* (*filled circles*), RVD took place in 100 mOsm trehalose medium, but it vanished in galactose medium of the same osmolality (Fig. 2*B*). Similar to galactose, 100 mOsm solutions of other *monomeric* sugars and sugar alcohols inhibited partially (*ino*) or completely (*glu*, *sor*) RVD in Jurkat cells. In contrast, the cells retained their ability to undergo RVD in all hypotonic solutions containing a di- or trisaccharide (*suc*, *tre* or *raf*) as the major osmolyte (*see* Table 1).

The anion channel blocker NPPB (100 μM) strongly inhibited RVD in Jurkat cells exposed to 100 mOsm trehalose (Fig. 2*A*, *triangles*) and also the partial RVD in 100 mOsm inositol (*see* below), suggesting the involvement of anion channels in the RVD of Jurkat cells in hypotonic sugar solutions. DIDS (1 mM) was less efficient at blocking RVD (Fig. 2*A*, *squares*). Much higher concentrations of the cation channel blocker Ba^{2+} (~10 mM) were required to noticeably inhibit the RVD of Jurkat cells in 100 mOsm trehalose. These findings are in agreement with earlier electrophysiological and isotope flux studies, which have shown that swelling-activated currents and solute transport are inhibited by a range of anion channel blockers, but are less sensitive to Ba^{2+} [10, 14, 18, 32].

Numeric Simulations of the VSC Model

The complex volumetric response of Jurkat cells to hypotonic stress was analyzed with the volume-sensitive channel (VSC) model outlined in the Appendix. The VSC model is based on the simplest L_p-P formalism (Eqs. A1–A3), in which the hydraulic conductivity L_p, electrolyte P_e and sugar permeabilities P_s, are used to characterize the cell membrane (for review *see* [24]). In contrast to the usual approach, in which the membrane permeability is viewed as a constant parameter, the effective membrane permeability is treated as a function of the relative cell volume in the VSC model. In Eqs. A2 and A3, the volume dependences of electrolyte and sugar permeability are given by the terms $\phi_{e,s} \times P_{e,s}^{max}$. The "swelling activation" factor for sugars, ϕ_s, was assumed to be equal to that of electrolyte ϕ_e (i.e., $\phi_s = \phi_e = \phi$). The dependence of ϕ on v is given by Eq. A4 (Appendix) and illustrated graphically by the inset in Fig. 4*A*.

To demonstrate that the VSC model is appropriate for analyzing the experimental volumetric data of Jurkat cells under acute hypotonic stress a number of numerical simulations were first performed with the model. The curves in Fig. 4 illustrate the relative volume versus time responses (*v vs. time*) of a hypothetical cell, calculated with Eqs. A1–A4 (Appendix) using *Mathematica*. Curves *1*, *2*, *3*, etc., in Fig. 4*A*, 4*B* and 4*C* were computed by incrementing individually L_p, P_e^{max} and P_s^{max}, respectively, while other parameters remained unchanged, as stated in the figure legend. In Fig. 4*D*, two parameters, i.e., extracellular sugar and electrolyte osmolalities (C_s^o and C_e^o, respectively), were changed in order to keep the total external osmolality constant ($C_s^o + C_e^o = 100$ mOsm), in accordance with the experimental conditions of this study. The symbols for further parameters used in the VSC model are defined in Table 2.

Inspection of the theoretical plots reveals that the initial portion of the $v(t)$ curves (i.e., the initial cell swelling due to the fast water inflow) is dominated by the hydraulic conductivity L_p. Thus, increasing L_p causes the cell to swell faster and raises the initial swelling magnitude v_{max} (Fig. 4*A*, curves *1–5*). In contrast, the secondary volume changes, i.e., the intermediate and final portions of the v curves, are largely determined by both solute permeabilities, P_s^{max} and P_e^{max}, as well as by their ratio. Varying either P_e^{max} or P_s^{max} has little effect on the initial swelling phase, but strongly influences the secondary volume changes (Figs. 4*B* and 4*C*). For P_s^{max} less than P_e^{max}, complete or partial RVD occurs (Fig. 4*C*,

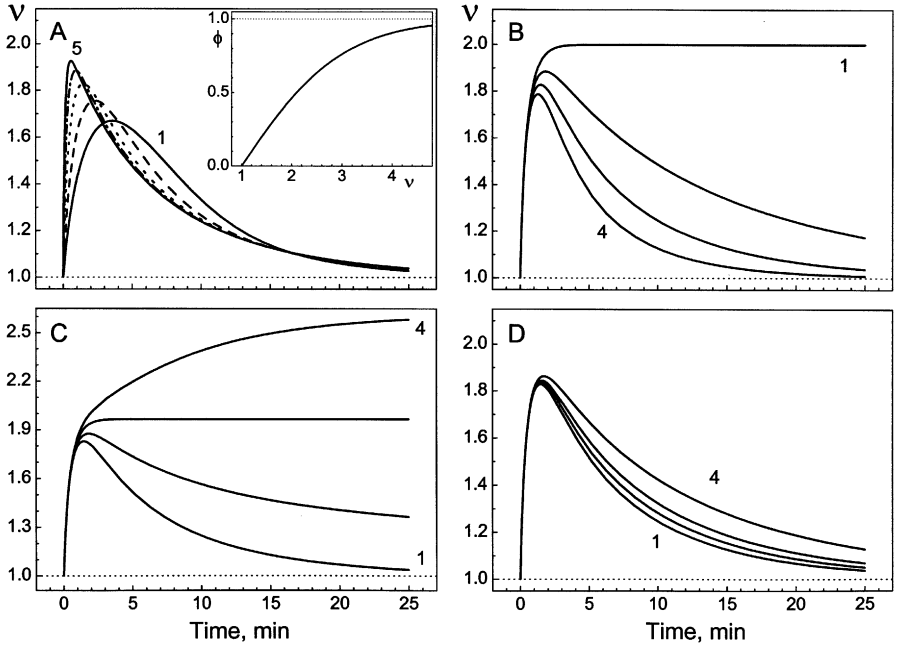

Fig. 4. Numerical simulations of the temporal volume changes calculated with the VSC model given in the Appendix by Eqs. A1–A4. The hypothetical cell was exposed to an acute hypotonic challenge (100 mOsm) at time zero. The simulations were performed with the following common parameters: the isotonic cell radius to $r_0 = 8$ μm, the osmotically inactive relative cell volume $v_b = 0.5$; the initial intracellular osmolalities for electrolyte C_e^i ($t = 0$) = 300 mOsm and sugar C_s^i ($t = 0$) = 0. The inset in *A* illustrates the dependence of the open ratio parameter ϕ on the relative cell volume v, given by Eq. A4 (Appendix). In *A–C*, the extracellular solute osmolalities after medium exchange ($t > 0$) were $C_s^o = 100$ mOsm and $C_e^o = 0$. (*A*) Curves *1–5* were calculated for $L_p = (0.65, 1.3, 2.6, 5.2 \text{ and } 10.4) \times 10^{-13}$ $m^3N^{-1}s^{-1}$, respectively. The solute permeabilities were constant: $P_e^{max} = 10^{-8}$ m s^{-1}, $P_s^{max} = 0$. (*B*) Curves *1–4* were calculated for $P_e^{max} = (0, 0.5, 1.0, 1.5) \times 10^{-8}$ m s^{-1}, respectively, whereas $P_s^{max} = 0$ and $L_p = 2.6 \times 10^{-13}$ $m^3N^{-1}s^{-1}$ were constant. (*C*) Curves *1–4* were calculated for $P_s^{max} = (0, 0.5, 1.0, 1.5) \times 10^{-8}$ m s^{-1}, respectively, whereas $P_e^{max} = 10^{-8}$ m s^{-1} and $L_p = 2.6 \times 10^{-13}$ m^3 $N^{-1}s^{-1}$ were constant. (*D*) The curves were calculated for various extracellular sugar and electrolyte osmolalities, while keeping the total osmolality of 100 mOsm unchanged. Curves *1–4* correspond to the following osmolal ratios of sugar/electrolyte: 0/100, 10/90, 20/80 and 40/60, respectively. $P_e^{max} = 10^{-8}$ m s^{-1}, $P_s^{max} = 0$, and $L_p = 2.6 \times 10^{-13}$ $m^3N^{-1}s^{-1}$ were constant. Note that curves *A3*, *B3*, *C1* and *D1* are identical.

Table 2. Definitions of the major symbols

Symbols	Description	Units	Value
0	Subscript 0 represents original isotonic values		
e, *s*	Subscripts: *e*, electrolyte; *s*, sugar (carbohydrate)		
i, *o*	Superscripts: *i*, intracellular; *o*, extracellular		
A	Cross-section or projected cell area	μm^2	Measurable parameter
r (r_0)	Cell radius (isotonic cell radius at 300 mOsm)	μm	$r = (A/\pi)^{0.5}$
S	Apparent cell surface area	μm^2	Assumed invariable $S = 4\pi r_0^2$
V and $V_0 = V_{iso}$	Cell volume and original isotonic volume at 300 mOsm	μm^3	$V = 4\pi r^3/3$
v	Relative cell volume		$v = V/V_0$
v_b	Osmotically inactive cell volume portion at 300 mOsm		
C_e^i and C_e^o	Intra- and extracellular osmolality of electrolytes	osmol/kg	
C_s^i and C_s^o	Intra- and extracellular osmolality of sugars	osmol/kg	
L_p	Hydraulic conductivity	$m^3N^{-1}s^{-1}$	
P and P^{max}	Solute permeability and its maximum value	m s^{-1}	$P = \phi \times P^{max}$ (*see* Eq. A4)
ϕ	Volume-dependent channel activity factor		$0 \le \phi \le 1$, Eq. A4
R	The universal gas constant	J mol^{-1} K^{-1}	8.31
T	Temperature	K	298
t	Time	s	Variable

curves *1* and *2*). If P_s^{max} is equal to or larger than P_e^{max}, RVD vanishes (Fig. 4*B*, curve *1*; Fig. 4*C*, curves *3* and *4*). Moreover, if $P_s^{max} > P_e^{max}$, the cell exhibits secondary swelling, but with a much lower rate (Fig. 4*C*, curve *4*) than during the initial swelling. Figure 4*D* shows that increasing the external elec-

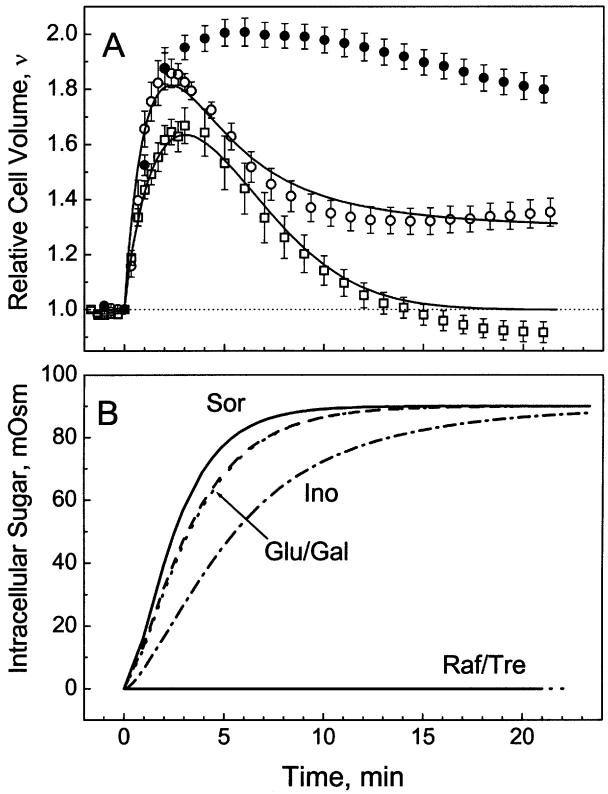

Fig. 5. (*A*) Time courses of the relative volume of Jurkat cells in hypotonic raffinose and inositol solutions (*empty squares* and *circles*, respectively). Note that, in contrast to other monomeric carbohydrates (Fig. 2 and Table 1), 100 mOsm inositol *partially* inhibited RVD in Jurkat cells. The continuous curves in *A* are the best fits of the VSC model to the data. The fitted parameters are given in Table 3. 100 μM NPPB inhibited the partial RVD in 100 mOsm inositol (*filled circles* in *A*). (*B*) The various curves show the temporal changes in the intracellular osmolality of indicated carbohydrates. The curves were calculated using the VSC model and the fitted parameters given in Table 3.

trolyte content, while keeping the total osmolality of external medium constant, alters only slightly the time course of RVD in the presence of impermeable sugar ($P_s = 0$). Comparison of the simulated curves (Fig. 4) with the experimental data (Fig. 2) shows that the VSC model describes well the complexity of the cell volume excursions in the presence of different sugars.

Volumetric Data Analysis

Best least-square approximations of the VSC model to the volumetric data (continuous curves in Fig. 2 and Fig. 5*A*) were calculated using a numeric nonlinear regression (NNLR) procedure. In general, the VSC model contains three unknown parameters: L_p, P_e^{max} and P_s^{max}. All other quantities appearing in the model are known. In 100 mOsm media, the extracellular sugar and electrolyte osmolalities were C_s^o = 90 mOsm and C_e^o = 10 mOsm, respectively. The 200 mOsm solutions contained 190 mOsm carbohydrate and 10 mOsm electrolyte. The original isotonic cell volume V_0 and cell surface S_0 (assumed invariable) were determined microscopically (Fig. 1). The osmotically inactive volume ratio v_b was determined from the Boyle van't Hoff plot (Fig. 3). The time-dependent relative cell volume $v(t)$ was the fitted variable.

From the best fits of the VSC model to the volumetric data of individual cells, the membrane transport parameters L_p, P_e^{max} and P_s^{max} were deduced for each individual cell. Table 3 summarizes the mean values (± SE) of the membrane parameters of Jurkat cells exposed to 200 and 100 mOsm solutions of various carbohydrates. At a given medium osmolality (e.g., 100 mOsm), the highest P_e^{max} values for electrolyte were observed in the presence of sorbitol (5.7×10^{-8} m s^{-1}) and galactose (4.3×10^{-8} m s^{-1}). Substitution of a monomeric solute by an oligosaccharide slightly reduced P_e^{max} to $(2.2–3.5) \times 10^{-8}$ m s^{-1}. At 200 mOsm, the P_e^{max} value varied only slightly among various carbohydrate solutions (Table 3), suggesting that sugar substitution did not noticeably affect the swelling-activated electrolyte efflux. Under mild hypotonic stress, the fitted P_e^{max} values for electrolyte were greater by 3–4 orders of magnitude than the corresponding P_s^{max} values. This means that the permeabilities of all carbohydrates were negligible at 200 mOsm ($P_s^{max} \approx 0$, Table 3).

In contrast to L_p and P_e^{max}, which were practically unaffected by variations of medium tonicity, the P_s^{max} values of monomeric sugars and sugar alcohols were strongly dependent on the osmolality. Thus, reduction of the osmolality from 200 to 100 mOsm resulted in a dramatic increase of the P_s^{max} values of monomeric carbohydrates from zero to $(1.7–5.7) \times 10^{-8}$ m s^{-1}, whereas the permeabilities of di- and trisaccharides remained very low (Table 3).

Intracellular Sugar

Using the fitted values of L_p, P_s^{max} and P_e^{max} (Table 3), the time courses of sugar uptake by hypotonically stressed cells can be calculated from the volumetric data by applying the VSC model (Eq. A3). The theoretical plots of the C_s^i versus time (Fig. 5*B*) illustrate that *gal*, *glu* and *sor* accumulated rapidly in Jurkat cells, reaching the maximum C_s^i value (~90 mOsm) within few minutes (5–7 min) after exposure to 100 mOsm medium. Inositol entered the cells somewhat slower than other monomeric osmolytes (Fig. 5*B*), but its osmolality also reached a high value of about 85 mOsm after 20–25 min incubation. In contrast, accumulation of oligosaccharides (*tre*, *raf* and *suc*) in Jurkat cells was negligible within the observation time interval.

Table 3. Membrane parameters of Jurkat cells exposed to hypotonic media of different osmolalities and carbohydrate composition[1]

Carbohydrate	N	L_p m^3 N^{-1} s^{-1}	P_e^{max} m s^{-1}	P_s^{max} m s^{-1}
200 mOsm, mild hypotonic stress				
Galactose	4	$(11.2 \pm 0.8) \times 10^{-14}$	$(3.3 \pm 0.8) \times 10^{-8}$	~0
Glucose	5	$(5.4 \pm 0.3) \times 10^{-14}$	$(5.2 \pm 0.6) \times 10^{-8}$	~0
Sorbitol	7	$(8.2 \pm 0.8) \times 10^{-14}$	$(3.2 \pm 0.4) \times 10^{-8}$	~0
Inositol	5	$(7.2 \pm 0.6) \times 10^{-14}$	$(5.1 \pm 0.6) \times 10^{-8}$	~0
Trehalose	3	$(6.4 \pm 0.9) \times 10^{-14}$	$(3.9 \pm 0.3) \times 10^{-8}$	~0
100 mOsm, strong hypotonic stress				
Galactose	7	$(8.2 \pm 1.3) \times 10^{-14}$	$(4.3 \pm 1.2) \times 10^{-8}$	$(4.0 \pm 1.3) \times 10^{-8}$
Glucose	5	$(11.0 \pm 2.9) \times 10^{-14}$	$(4.2 \pm 1.4) \times 10^{-8}$	$(3.8 \pm 1.3) \times 10^{-8}$
Sorbitol	9	$(9.2 \pm 0.7) \times 10^{-14}$	$(5.7 \pm 0.5) \times 10^{-8}$	$(5.7 \pm 0.5) \times 10^{-8}$
Inositol	6	$(11.2 \pm 1.4) \times 10^{-14}$	$(3.9 \pm 0.2) \times 10^{-8}$	$(1.7 \pm 0.2) \times 10^{-8}$
Sucrose	5	$(10.6 \pm 2.6) \times 10^{-14}$	$(3.5 \pm 0.4) \times 10^{-8}$	~0
Trehalose	5	$(16.2 \pm 0.3) \times 10^{-14}$	$(2.2 \pm 0.2) \times 10^{-8}$	~0
Raffinose	5	$(9.2 \pm 1.1) \times 10^{-14}$	$(2.9 \pm 0.3) \times 10^{-8}$	~0

[1]The data represent the means ± SE of N cells. L_p, P_e^{max} and P_s^{max} are defined in Table 2.

In order to verify the C_s^i values calculated from the volumetric data (Fig. 5*AB*), intracellular carbohydrates were determined directly by chromatography. In this series of experiments, cell samples were incubated for 25 min in 100 mOsm solutions of trehalose, inositol or sorbitol, as well as in hypotonic PBS diluted to the same osmolality (control). Prior to chromatography, the hypotonically treated cells were collected and solubilized (*see* above, Materials and Methods). The sugar composition and content were analyzed in cell lysates by means of high performance anion-exchange chromatography (HPAEC) with pulsed amperometric detection (PAD).

Figure 6 shows representative chromatograms of cell lysates that were prepared from cells pretreated with different hypotonic solutions: PBS, trehalose, inositol and sorbitol (*A–D*, respectively). The retention times (RT) for trehalose, inositol and sorbitol, whose peaks were well resolved in the chromatograms, were 15.3, 8.3, and 16.1 min, respectively. In the lysates of control cells (Fig. 6*A*), a small amount of inositol was detected (the peak PAD values of ~3.5 nC with RT of 8.3 min). From the chromatograms obtained in 3 independent experiments, the cytosolic concentration of inositol in control cells was found to be 1.0 ± 0.1 mM (mean ± SE). For these calculations, the electronic cell volume and density, as well as corresponding calibration PAD-curves were used. The inositol levels in cells exposed to hypotonic trehalose and sorbitol solutions (Figs. 6*B* and 6*D*) were similar to that in control. It is interesting to note that the background concentration of inositol in control Jurkat cells determined here by HPAEC compares favorably to the value of 1.29 ± 0.15 mM detected by ^{1}H-NMR in human blood lymphocytes [49].

Exposure of cells to hypotonic inositol or sorbitol solutions resulted in dramatic increase of both sugar alcohols in the cell lysates (Figs. 6*C* and Fig 6*D*, the peak PAD values of ~800 and ~250 nC). Using chromatographic and electronic size data, the cytosolic concentrations of 76 ± 7 and 63 ± 2 mM (N = 3) were calculated for inositol and sorbitol, respectively. These findings indicate significant uptake of both monomeric sugar alcohols during hypotonic treatment, thus validating the theoretical estimates based on the volumetric data analysis (Fig. 5*B*).

As expected, HPAEC-PAD did not reveal any detectable amounts of trehalose in control and in the cell samples treated with either sugar alcohol (Figs. 6*A*, 6*C* and 6*D*), whereas the chromatograms of trehalose-treated cells displayed a detectable trehalose peak with an RT = 16.1 min and a magnitude of about 6 nC (Fig. 6*B*). Based on these data, a concentration of 9.4 ± 2.2 mM was calculated for the intracellular trehalose, which exceeded markedly the value deduced from the volumetric data (Fig. 5*B*). A larger trehalose concentration measured by chromatography can be explained by the contamination of cell lysates with extracellular trehalose, e.g., due to sugar adsorption to the cell surface. Strong interactions of trehalose with phospholipid membrane have been reported elsewhere [1]. In addition, trehalose uptake can also occur via the fluid-phase endocytosis [52] without involvement of swelling-activated pathways. Even though the HPAEC and volumetric estimates of the intracellular trehalose were different, the chromatographic data confirmed the theoretical prediction that the swelling-activated uptake of trehalose occurred much more slowly than those of inositol and sorbitol.

Cell Viability and Proliferation after Hypotonic Treatment

Typical RF distributions of untreated control, hypotonically treated and saponin-lysed Jurkat cells

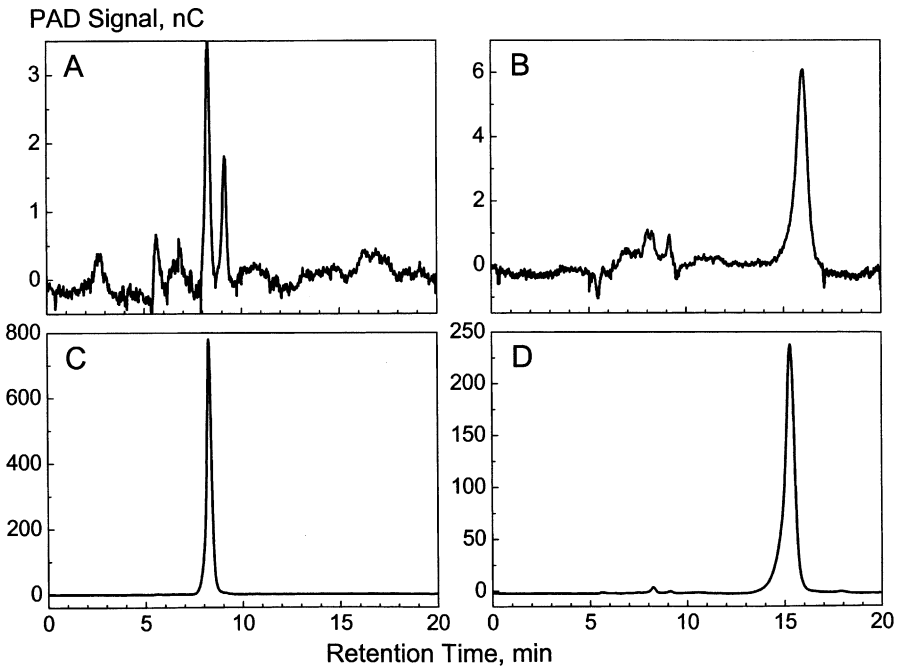

Fig. 6. Typical HPAEC-PAD chromatograms of Jurkat cell lysates: the data in *A–D* represent the cell samples treated, respectively, with hypotonic PBS, trehalose, inositol and sorbitol solutions of the same osmolality of 100 mOsm. The chromatograms show the PAD responses in nC as functions of time after starting the elution.

suspended in the presence of 40 μM PI are shown in Fig. 7. The histogram of the control cells (Fig. 7, curve *1*) exhibited a very weak fluorescence peak centered at about 7 arbitrary units (a.u.). Usually, only a small fraction (~2%) of control cell samples showed RF intensities larger than 500 a.u. after staining with PI. This subpopulation consists of dead cells, as demonstrated by the addition of 0.2% saponin. Cells lysed with saponin showed a very high RF intensity level ranging from about 500 to 2000 a.u. (Fig. 7, curve *4*), which corresponded to near saturation of the intracellular binding sites for PI [31].

The RF distributions of cells treated with 100 mOsm glucose and sorbitol solutions (Fig. 7, curves *2* and *3*, respectively) were similar to that of control (Fig. 7, curve *1*). The strong hypotonic treatment only slightly shifted the main RF peak from 7 a.u (control) to ~10 a.u., associated with the appearance of a small fraction of cells (~6–22%) with an increased PI content ($20 < RF < 300$ a.u.). The level of PI was, however, far from equilibrium with the medium, indicating that these cells were still viable. The portions of strongly fluorescent, dead cells (~1–3% at $RF > 500$ a.u.) after treatment with hypotonic glucose and sorbitol solutions were comparable to that in control. Qualitatively similar PI content distributions were obtained for cell samples exposed to 100 mOsm galactose and inositol media (*data not shown*). The results of the PI exclusion assay presented in Fig. 7 demonstrate that the majority of Jurkat cells were capable of withstanding an extensive hypotonic shock without significant membrane damage.

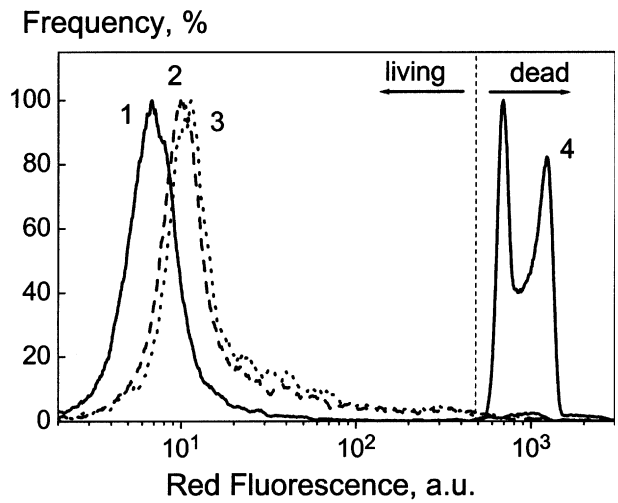

Fig. 7. Representative red fluorescence (RF) histograms of Jurkat cells in the presence of 40 μM PI. Curve *1* shows the RF signals of untreated control cells. Histograms *2* and *3* represent, respectively, cell samples exposed to 100 mOsm hypotonic glucose and sorbitol for 25 min. Curve *4* represents saponin-treated cells. Note that only a small fraction of hypotonically treated cells (~1–3%) was damaged, i.e., exhibited strong fluorescence signals above 500 a.u.

We also examined the proliferation activity of hypotonically treated Jurkat cells by means of electronic cell counting. Figure 8 shows cell growth curves generated from sequential cell counting assays in untreated control (*filled circles*) and hypotonically treated cell samples (*empty symbols*). Control cells exhibited a characteristic lag phase (days *0–1*), followed by a rapid growth phase (days *2–7*) and a subsequent plateau phase. In the case of hypotonic

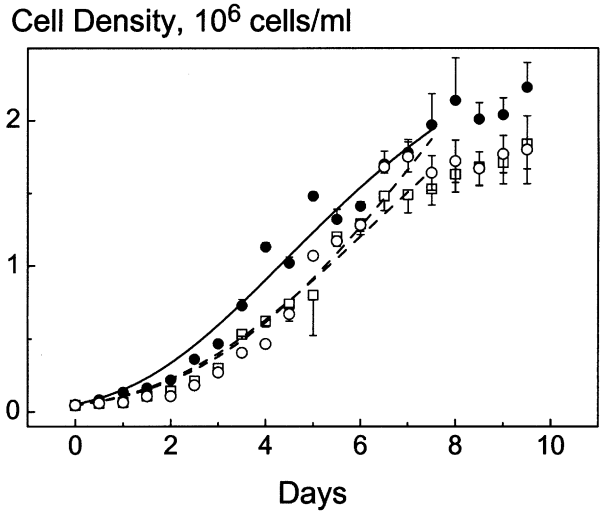

Fig. 8. Proliferation of Jurkat cells treated with hypotonic glucose and inositol solutions (100 mOsm, 25 min, *empty circles* and *squares*, respectively), compared to control (*filled circles*). Each data point represents the mean ± SE of triplicate measurements, using electronic cell counting. The smooth curves show the best least-square fits of the Gompertz equation (*see* Materials and Methods) to the data.

100 mOsm solutions of *glu* and *ino*, the lag phase was extended to about 1.5–2 days (Fig. 8, *empty squares* and *circles*, respectively), presumably due to the loss of cytosolic electrolytes through swelling-activated channels. Despite the prolonged lag phase, the initial growth rates in hypotonically treated cell samples (α/β = 4.4–4.9) were similar to that in control (α/β = 4.1), as demonstrated by fitting the Gompertz equation to the data (*see* Materials and Methods). The effects of 100 mOsm galactose and sorbitol on cell growth (*data not shown*) were similar to those of glucose and inositol.

In the light of the results presented in Figs. 7 and 8 it is clear that the majority of Jurkat cells remained viable and were able to proliferate after a severe hypotonic challenge in 100 mOsm monosaccharide solutions. These findings are consistent with a bulk of literature published on electrofusion and electrotransfection of cells, which are routinely performed in strongly hypo-osmolar, sugar-substituted media (for review *see* Ref. 55). There is also evidence [17] that apoptosis of cells is greatly reduced when electrolytes are replaced by sugars.

Discussion

In this study, the time courses of cell volume changes were measured in Jurkat cells following their exposure to a hypotonic solution containing a mono- or an oligosaccharide as the major osmolyte. Analysis of the volumetric data with the theoretical model developed here (VSC model, Appendix) allowed the evaluation of the membrane transport parameters in terms of hydraulic conductivity (L_p) and volume-dependent permeability coefficients for sugar and electrolyte. Based on these parameters the kinetics of sugar uptake by cells during hypotonic stress could be derived.

Hydraulic Conductivity

The rapid water influx into cells suddenly exposed to hypotonic stress gave rise to a fast initial swelling. At a given osmolality, neither swelling kinetics nor magnitude (*see* v_{max} and T_{max} in Table 1) were noticeably affected by the type of carbohydrate used as the major external osmolyte. Therefore, cell surface structures, such as glycocalyx, microvilli, etc., which can alter the actual solute gradients via unstirred layer and related effects [16], did not, apparently, significantly influence the passive water influx into Jurkat lymphocytes.

The initial swelling is largely determined by L_p, which in turn is directly related to the osmotic water permeability P_f. The latter is defined as $P_f = RTL_p/\upsilon_w$, where R, T and υ_w are the gas constant, temperature and partial molar volume of water (υ_w = 18 cm^3/mol), respectively. The L_p values of (5.4–16.2) × 10^{-14} m^3 N^{-1} s^{-1}(Table 3) (or 0.32–0.97 μm min^{-1} bar^{-1}) found here for Jurkat cells and the corresponding P_f estimates (7.4–22.3) × 10^{-6} m s^{-1} are in good agreement with previously reported data for this cell line and other human cells. Thus, the P_f values of (9.3 ± 4.8) × 10^{-6} and 12 × 10^{-6} m s^{-1} exhibited by Jurkat cells and by red blood cells, respectively [30, 37], are both within the P_f range obtained in the present study. It is noteworthy that all P_f values derived here are at least one order of magnitude less than the cutoff value P_f = 10^{-4} m s^{-1}, which is viewed as a criterion for the presence of aqueous pores in cell membranes [50].

The L_p values of (8.2–16.2) × 10^{-14} m^3 N^{-1} s^{-1} obtained in 100 mOsm solutions of various sugars (except for trehalose) differed only slightly from the L_p of (5.4–11.2) × 10^{-14} m^3 N^{-1} s^{-1} measured at 200 mOsm (Table 3), suggesting that, in general, sugar concentration had little effect on the water influx. In the case of trehalose, however, increasing osmolality from 100 to 200 mOsm resulted in a nearly threefold L_p decrease. The stronger effect of trehalose may be due to the unique ability of this sugar to interact with biological membranes via hydrogen bond formation with the phospholipid head groups [1].

RVD and Uptake of Carbohydrates

Unlike the initial swelling phase, the direction and magnitude of the *secondary* volume changes of Jurkat

cells during hypotonic stress were found to depend strongly on both osmolality and molecular size of the carbohydrate (Figs. 2 and 5, Table 1).

In response to a mild osmotic shift from 300 to 200 mOsm, Jurkat cells underwent complete RVD in the presence of all sugars and sugar alcohols studied here. Analysis of the volumetric data with the VSC model revealed that the initial cell swelling in 200 mOsm solutions rendered the cell membrane permeable to electrolyte (Table 3, $P_e^{max} > 0$). In contrast to electrolyte permeability, the membrane permeability to sugars and sugar alcohols remained very poor ($P_s^{max} \approx 0$). It seems that, in spite of the volume regulatory release of electrolyte, the small initial swelling of 10–20% at 200 mOsm ($v_{max} \approx 1.2$, Table 1) was not sufficient to activate sugar-conducting pathways in the Jurkat cell membrane. As discussed below, at stronger hypotonicity (i.e., 100 mOsm), the transport of electrolyte and monomeric carbohydrates may occur through the same swelling-activated channels. In this case, the strong osmolality dependence of the relative sugar-to-electrolyte permeability (P_s^{max}/P_e^{max}, Table 3) suggests that the osmotic thresholds at which these channels are activated should be different for sugars and electrolyte. It is interesting to note that, unlike Jurkat lymphocytes, HeLa cells show a significant increase in the influx rate of sorbitol and other solutes, such as taurine, thymidine, etc., upon reduction in the osmolality from 300 to 200 mOsm [14].

Similar to their response to the mild 200 mOsm stress, Jurkat cells were also able to accomplish RVD in strongly hypotonic solutions of di- and trisaccharides tested here (100 mOsm, Table 1). This means that membrane permeability to oligosaccharides remained very poor (Table 3), even though the initial cell swelling at 100 mOsm was much larger than at 200 mOsm.

In sharp contrast to the 200 mOsm stress as well as to 100 mOsm *oligosaccharide* media, strongly hypotonic solutions (100 mOsm) of *monomeric* sugars and sugar alcohols inhibited RVD partially (*ino*) or completely (*gal*, *sor*, *glu*). Theoretical analysis of these data showed that the cell membrane became highly permeable to all monomeric carbohydrates (Table 3) and that efficient uptake of these solutes by cells occurs within few minutes at 100 mOsm (Fig. 5*B*). In agreement with the volumetric data, HPAEC analysis also revealed high millimolar concentrations of inositol and sorbitol in the cytosol of hypotonically treated Jurkat cells (Fig. 6), whereas intracellular trehalose level was much lower. Despite the strong hypotonic shock, the majority of Jurkat cells survived and were able to proliferate in culture after exposure to 100 mOsm solutions (Figs. 7 and 8).

Taken together, the volumetric data analysis and chromatographic sugar determination suggest that RVD inhibition by monomeric sugars and sugar alcohols can be viewed as an indication of the swelling-activated uptake of these small solutes by cells through volume-sensitive channels. This conclusion is consistent with the results of earlier studies, in which permeability of mammalian cell membranes to a series of organic and inorganic anions was examined under anisotonic conditions. Thus, similar to the neutral monomeric carbohydrates studied here, large poorly permeable anions, such as gluconate, allow a volume decrease in hypotonically swollen human lymphocytes, whereas highly permeating small inorganic anions, such as SCN^- and I^-, inhibit RVD or even induce secondary swelling [11].

Similar to T-lymphocytes studied here and elsewhere [37], many other cell and tissue types, including hepatocytes [15], kidney cells [21], astrocytes [18], Ehrlich ascites tumor cells [35] etc., undergo RVD after transient initial swelling induced by an acute hypotonic challenge. Recent studies have demonstrated that RVD is not simply the controlled release of inorganic ions (primarily K^+ and Cl^-) but it also involves swelling-mediated efflux of small organic osmolytes, such as amino acids, methyl-amines and sugar alcohols. As already mentioned, organic osmolytes can make a significant contribution to the total intracellular osmolality, especially if cells are grown in hyperosmotic media [21, 22]. It is noteworthy that unlike inorganic ions and urea, which, at high concentrations, destabilize protein structure, sugar alcohols and some other organic osmolytes do not interfere with protein functions even when present at high concentrations [15, 22, 53]. Based on their stabilizing effect on macromolecules and membranes, sugar alcohols and some other organic osmolytes protect living cells against extreme temperatures and desiccation [27].

Various volume-sensitive transport pathways (including anion and cation channels) are involved in the volume regulation in osmotically stressed cells. A large body of evidence now indicates that in many cell types the volume regulatory efflux of structurally dissimilar organic osmolytes from swollen cells occurs via the volume-sensitive organic osmolyte and anion channel (VSOAC) [19, 46]. Arguments in support of the hypothesis that anion-selective channels provide a major route for the volume-regulatory efflux of organic osmolytes from vertebrate cells are presented in detail elsewhere [23]. Volume-sensitive channels are commonly found in a variety of animal species, including mammals, amphibians, etc. [22, 45]. Similar mechanisms may also be involved in the osmoregulation of hypotonically challenged plant cells [16]. The large effect of the anion channel blocker NPPB observed in the present study (Figs. 2*A* and 5*A*) also indicates the involvement of anion channels in the RVD response of Jurkat cells to strong hypotonic sugar solutions.

Selective Permeability of Swelling-Activated Channels

In the present study, the osmotic shift from 200 to 100 mOsm caused an increase of the initial cell swelling v_{max} from ~1.2 to ~1.9 (Table 1), which was accompanied by a dramatic increase of the membrane permeability to monosaccharides (Table 3). The much greater swelling magnitude at 100 mOsm appears to be the reason for the activation of volume-sensitive pathways conducting monomeric sugars and sugar alcohols. Judging by the P_s^{max} values given in Table 3, the permeability of monosaccharides approached that of electrolyte in cells exposed to 100 mOsm stress. In the presence of an inward sugar gradient (i.e., under the conditions of our experiments), the monosaccharide influx obviously abolished RVD by compensating the loss of intracellular solutes from osmotically swollen Jurkat cells. Our finding that monosaccharide permeability was higher at lower osmolality (Table 3) is consistent with the observation that the rate constant of ^{3}H-inositol efflux from rat astrocytes increases with decreasing osmolality [18].

Despite extensive swelling at 100 mOsm, the membrane of Jurkat cells remained poorly permeable to the larger molecules of di- and trisaccharides (*tre*, *suc* and *raf*), all of which allowed complete RVD at 100 mOsm and even at a more severe hypotonic shift (e.g., 50 mOsm trehalose, *data not shown*). Unlike Jurkat cells studied here, some cell types (e.g., HeLa and renal epithelial cells) show swelling-activated transport of oligosaccharides including sucrose and raffinose [42].

Analysis of the volumetric response of Jurkat cells to 100 mOsm stress revealed that the swelling-activated permeability to monomeric sugar and sugar alcohols decreased in the order: *sor* > *gal* ≈ *glu* > *ino* (Table 3). The P_s^{max} value for sorbitol was found to be larger by about a factor of three than that for inositol (570 *vs.* 170 μm/s, respectively). This finding is in good agreement with the results on osmotically swollen renal epithelial cells, in which the permeability of sorbitol is 2.7 times that of inositol, as determined by comparing the relative rates of solute release in isotope flux studies [42]. Furthermore, measurements of the swelling-activated efflux of organic osmolytes (e.g. *sor*, *ino*, taurine, etc.) from renal medullary cells have shown that the osmotic threshold and steepness of the activation curve are different for various osmolytes [21]. Thus, the swelling-activated efflux of inositol from these cells has a much longer lag period after a hypotonic challenge than sorbitol release [21]. A longer lag time required for activation of inositol permeability would also account for its slower uptake by Jurkat cells reported here (Fig. 5*B*). If carbohydrate molecules are viewed as cylinders, the lower permeability of the cyclic polyol inositol may be due to its larger cylindrical diameter of 5.9 Å compared to the 5.0 Å of the linear polyalcohol sorbitol [46]. Besides the molecular-size effect, the permeation rate of organic osmolytes through swelling-activated pathways also depends on the arrangement of OH-groups in the molecule [22].

Concluding Remarks

We have demonstrated that hypotonic treatment is an efficient method for the loading of human lymphocytes with high concentrations of low-molecular weight solutes including monomeric sugars and sugar alcohols. In contrast to most invasive techniques currently used for the delivery of membrane-impermeable cryo- and lyoprotectants into cells, our method utilizes the dormant transport mechanisms naturally present in the cell membrane, most likely, the swelling-activated pathways known in the literature as the volume-sensitive organic osmolyte and anion channels [19]. Preliminary studies have shown that monomeric sugar alcohols could also easily be introduced through swelling-activated channels into human blood dendritic cells as well as into whole organs such as isolated rat islets of Langerhans, supporting the view that volume-sensitive channels are nearly ubiquitous in animal cells [22, 45]. Therefore, the method presented here appears to be a promising approach for the rapid delivery of small carbohydrate molecules and other potential stabilizers of cellular macromolecules and membranes into a variety of cell and tissue types. In combination with conventional membrane-permeable cryoprotectants, such as dimethylsulfoxide, glycerol, etc. [2, 8], high intracellular levels of carbohydrates can pave the way to significantly improve the survival of cryo- and lyopreserved cells. Finally, the method presented here is compatible not only with conventional cryoconservation but also with the novel miniaturized cryobank technology [54], with far-reaching implications for cryo- and lyopreservation of rare and valuable mammalian cells and tissues.

We are very grateful to Dr. Stephen G. Shirley for carefully proofreading. This work was supported by grants from the Bundesministerium für Bildung und Forschung (BMBF-16SV1329/0 to U.Z., H.S. and V.L.S, as well as BMBF-16SV1366/0 and BMBF-03N8707 to H.Z.), a Novo Nordisk Research Grant (to M.M.W. and S.S.) and by the Stiftung Rheinland Pfalz für Innovation (386261/0525 to S.S. and M.M.W.).

Appendix

A standard set of equations relating the passive fluxes of water (J_v), electrolyte (J_e) and sugar (J_s) through the cell membrane to the extra- and intracellular

osmolalities of the solutes was used to analyze the volume regulation data:

$$J_v = \frac{d(v - v_b)}{Sdt} = -\frac{L_p RT[(C_e^o - C_e^i) + (C_s^o - C_s^i)]}{V_0} \quad (A1)$$

$$J_e = \frac{d[C_e^i(v - v_b)]}{Sdt} = \frac{P_e(C_e^o - C_e^i)}{V_0} \quad (A2)$$

$$J_s = \frac{d[C_s^i(v - v_b)]}{Sdt} = \frac{P_s(C_s^o - C_s^i)}{V_0} \quad (A3)$$

Explanations for the symbols, sub- and superscripts used in Eqs. A1–A3 are summarized in Table 2. The equations are based on the classic two-parameter model (L_p-*P*-model), by assuming that solutes and solvent are transported independently [24].

Regulatory volume decrease (RVD) observed here after the fast cell swelling in response to an acute hypotonic stress implies the involvement of volume-sensitive channels (VSCs) for electrolytes and sugars. The impact of VSCs on the solute fluxes through the membrane can be modeled by introducing the volume-dependent permeability coefficients $P_{e,s}(v)$:

$$P_{e,s} = \phi \times P_{e,s}^{max} = \frac{1 - \exp(-|v-1|)}{1 + \exp(-|v-1|)} \times P_{e,s}^{max} \quad (A4)$$

Where $\phi = \frac{1-\exp(-|v-1|)}{1+\exp(-|v-1|)}$ is the volume-dependent *channel activity factor*, which is assumed to be the same for sugar and electrolyte. Equation A4 implies that the permeability increases from zero if the cell swells or shrinks from its isotonic volume, thus allowing to describe both regulatory volume decrease and increase in response to hypo- and hypertonic stresses, respectively.

As illustrated by the plot ϕ *versus* v (inset in Fig. 4*A*), the value ϕ and so the effective membrane permeability ($P_{e,s} = \phi \times P_{e,s}^{max}$) are both zero under isotonic conditions, i.e., at $v = 1$. The ϕ value increases gradually with volume v and approaches unity at $v \rightarrow$ infinity (i.e., $\lim_{v\to\infty} \phi = 1$), which in turn causes the effective membrane permeability $P_{e,s}$ for solutes to assume its maximum values $P_{e,s}^{max}$. It should be noted that the assumption of gradual $P_{e,s}$ increase does not account for some important properties of volume-sensitive channels, such as their steep activation at a threshold volume, different lag-times of activation, etc., reported in the literature for some cellular systems (*see* Discussion). To account for all complex membrane and cytosolic processes, also including the time-dependent ion conductance, membrane potential and cytosolic Ca^{2+} changes, triggered by hypotonic cell swelling, more sophisticated models are required. Despite its simplicity, the present model matched well the observed volumetric behavior of hypoosmotically treated Jurkat cells (Figs. 2 and 5), thus allowing the quantitative estimation of membrane parameters in terms of solute and water permeabilities (Table 3).

References

1. Bárdos-Nagy, I., Galántai, R., Fidy, J. 2001. Effect of trehalose in low concentration on the binding and transport of porphyrins in liposome-human serum albumin system. *Biochim. Biophys. Acta* **1512:**125–134
2. Beattie, G.M., Crowe, J.H., Lopez, A.D., Cirulli, V., Ricordi, C., Hayek, A. 1997. Trehalose: A cryoprotectant that enhances recovery and preserves function of human pancreatic islets after long-term storage. *Diabetes* **46:**519–523
3. Cameron, D.A., Ritchie, A.A., Miller, W.R. 2001. The relative importance of proliferation and cell death in breast cancer growth and response to tamoxifen. *Eur. J. Cancer* **37:**1545–1553
4. Crowe, J.H., Crowe, L.M., Carpenter, J.F., Wistrom, C.A. 1987. Stabilization of dry phospholipid-bilayers and proteins by sugars. *Biochem. J.* **242:**1–10
5. Crowe, J.H., Crowe, L.M. 2000. Preservation of mammalian cells - learning nature's tricks. *Nat. Biotechnol.* **18:**145–146
6. Downey, G.P., Grinstein, S., Sue-A-Quan, A., Czaban, B., Chan, C.K. 1995. Volume regulation in leukocytes: Requirement for an intact cytoskeleton. *J. Cell. Physiol.* **163:**96–104
7. Eggermont, J., Trouet, D., Carton, I., Nilius, B. 2001. Cellular function and control of volume-regulated anion channels. *Cell Biochem. Biophys.* **35:**263–274
8. Eroglu, A., Russo, M.J., Bieganski, R., Fowler, A., Cheley, S., Bayley, H., Toner, M. 2000. Intracellular trehalose improves the survival of cryopreserved mammalian cells. *Nat. Biotechnol.* **18:**163–167
9. Eroglu, A., Toner, M., Toth, T.L. 2002. Beneficial effect of microinjected trehalose on the cryosurvival of human oocytes. *Fertil. Steril.* **77:**152–158
10. Fürst, J., Gschwentner, M., Ritter, M., Botta, G., Jakab, M., Mayer, M., Garavaglia, L., Bazzini, C., Rodighiero, S., Meyer, G., Eichmüller, S., Wöll, E., Paulmichl, M. 2002. Molecular and functional aspects of anionic channels activated during regulatory volume decrease in mammalian cells. *Pfluegers Arch. Eur. J. Physiol.* **444:**1–25
11. Grinstein, S., Clarke, C.A., Dupre, A., Rothstein, A. 1982. Volume-induced increase of anion permeability in human lymphocytes. *J. Gen. Physiol.* **80:**801–823
12. Grinstein, S., Rothstein, A., Sarkadi, B., Gelfard, E.W. 1984. Responses of lymphocytes to anisotonic media: Volume-regulating behavior. *Am. J. Physiol.* **246:**C204–C215
13. Guo, N., Puhlev, I., Brown, D.R., Mansbridge, J., Levine, F. 2000. Trehalose expression confers desiccation tolerance on human cells. *Nat. Biotechnol.* **18:**168–171
14. Hall, J.A., Kirk, J., Potts, J.R., Rae, C., Kirk, K. 1996. Anion channel blockers inhibit swelling-activated anion, cation, and nonelectrolyte transport in HeLa cells. *Am. J. Physiol.* **271:**C579–C588
15. Häussinger, D. 1996. The role of cellular hydration in the regulation of cell function. *Biochem. J.* **313:**697–710
16. Heidecker, M., Mimietz, S., Wegner, L.H., Zimmermann, U. 2003. Structural peculiarities dominate the turgor pressure response of the marine alga *Valonia utricularis* upon osmotic challenges. *J. Membrane Biol.* **192:**123–139
17. Hofmann, F., Ohnimus, H., Scheller, C., Strupp., W., Zimmermann, U., Jassoy, C. 1999. Electric field pulses can induce apoptosis. *J. Membrane Biol.* **169:**103–109

18. Isaacks, R.E., Bender, A.S., Kim, C.Y., Shi, Y.F., Norenberg, M.D. 1999. Effect of osmolality and anion channel inhibitors on myo-inositol efflux in cultured astrocytes. *J. Neurosci. Res.* **57:**866–871
19. Jackson, P.S., Strange, K. 1993. Volume-sensitive anion channels mediate swelling-activated inositol and taurine efflux. *Am. J. Physiol.* **265:**C1489–C1500
20. Junankar, P.R., Kirk, J. 2000. Organic osmolyte channels: A comparative view. *Cell. Physiol. Biochem.* **10:**355–360
21. Kinne, R.K.H. 1998. Mechanisms of osmolyte release. *In:* Cell Volume Regulation. Lang, F, editor. pp 34–49, Karger, Basel
22. Kirk, K. 1997. Swelling-activated organic osmolyte channels. *J. Membrane Biol.* **158:**1–16
23. Kirk, K., Strange, K. 1998. Functional properties and physiological roles of organic solute channels. *Annu. Rev. Physiol.* **60:**719–739
24. Kleinhans, F.W. 1998. Membrane permeability modeling: Kedem-Katchalsky vs a two-parameter formalism. *Cryobiology* **37:**271–289
25. KoŠtál, V., Nedvd, O., Šimek, P. 1996. Accumulation of high concentrations of myo-inositol in the overwintering ladybird beetle *Ceratomegilla undecimnotata*. *Cryo-Lett.* **17:**267–272
26. Lang, F. 1998. Cell Volume Regulation. Karger, Basel
27. Lang, F., Busch, G.L., Völkl, H. 1998. The diversity of volume regulatory mechanisms. *Cell. Physiol. Biochem.* **8:**1–45
28. Lange, K. 2000. Regulation of cell volume via microvillar ion channels. *J. Cell. Physiol.* **185:**21–35
29. Lee, S.C., Price, M., Prystowsky, M.B., Deutsch, C. 1988. Volume response of quiescent and interleukin 2-stimulated T-lymphocytes to hypotonicity. *Am. J. Physiol.* **254:**C286–C296
30. Lieb, W.R., Stein, W.D. 1986. Non-Stokesian nature of transverse diffusion within human red cell membranes. *J. Membrane Biol.* **92:**111–119
31. Müller, K.J., Sukhorukov, V.L., Zimmermann, U. 2001. Reversible electropermeabilization of mammalian cells by high-intensity, ultra-short pulses of submicrosecond duration. *J. Membrane Biol.* **184:**161–170
32. Nilius, B., Eggermont, J., Droogmans, G. 2000. The endothelial volume-regulated anion channel, VRAC. *Cell. Physiol. Biochem.* **10:**313–320
33. Obendorf, R.L. 1997. Oligosaccharides and galactosyl cyclitols in seed desiccation tolerance. *Seed Sci. Res.* **7:**63–74
34. Okada, Y. 1998. Cell Volume Regulation. The Molecular Mechanism and Volume Sensing Machinery. Elsevier, Amsterdam
35. Pedersen, S.F., Hoffmann, E.K. 2002. Possible interrelationship between changes in F-actin and myosin Π, protein phosphorylation, and cell volume regulation in Ehrlich ascites tumor cells. *Exp. Cell Res.* **277:**57–73
36. Puhlev, I., Guo, N., Brown, D.R., Levine, F. 2001. Desiccation tolerance in human cells. *Cryobiology* **42:**207–217
37. Ross, P.E., Garber, S.S., Cahalan, M.D. 1994. Membrane chloride conductance and capacitance in Jurkat T lymphocytes during osmotic swelling. *Biophys. J.* **66:**169–178
38. Sands, J.M. 1994. Regulation of intracellular polyols and sugars in response to osmotic stress. *In:* Cellular and Molecular Physiology of Cell Volume Regulation. Strange, K, editor. pp 133–144, CRC, Boca Raton, FL
39. Schmidt, E., Kromminga, A., Kürschner, M., Zimmermann, H., Katsen, A.D., Bröcker, E.-B., Zillikens, D., Zimmermann, U., Sukhorukov, V.L. 2003. Trehalose conserves expression of bullous pemphigoid antigen 180 during desiccation and freezing. *J. Immunol. Methods* **275:**179–190
40. Schneider, H., Manz, B., Westhoff, M., Mimietz, S., Szimtenings, M., Neuberger, T., Faber, C., Krohne, G., Haase, A., Volke, F., Zimmermann, U. 2003. The impact of lipid distribution, composition and mobility on xylem water refilling of the resurrection plant *Myrothamnus flabellifolia*. *New Phytol.* **159:**487–505
41. Shirakashi, R., Köstner, C.M., Müller, K.J., Kürschner, M., Zimmermann, U., Sukhorukov, V.L. 2002. Intracellular delivery of trehalose into mammalian cells by electropermeabilization. *J. Membrane Biol.* **189:**45–54
42. Siebens, A.W., Spring, K.R. 1989. A novel sorbitol transport mechanism in cultured renal papillary epithelial cells. *Am. J. Physiol.* **257:**F937–F946
43. Storey, K.B. 1997. Organic solutes in freezing tolerance. *Comp. Biochem. Physiol. A Physiol.* **117:**319–326
44. Strange, K., Morrison, R. 1992. Volume regulation during recovery from chronic hypertonicity in brain glial cells. *Am. J. Physiol.* **263:**C412–C419
45. Strange, K. 1994. Cellular and Molecular Physiology of Cell Volume Regulation. CRC, Boca Raton, FL
46. Strange, K., Jackson, P.S. 1995. Swelling-activated organic osmolyte efflux: A new role for anion channels. *Kidney Int.* **48:**994–1003
47. Sukhorukov, V.L., Arnold, W.M., Zimmermann, U. 1993. Hypotonically induced changes in the plasma membrane of cultured mammalian cells. *J. Membrane Biol.* **132:**27–40
48. Sukhorukov, V.L., Mussauer, H., Zimmermann, U. 1998. The effect of electrical deformation forces on the electropermeabilization of erythrocyte membranes in low- and high-conductivity media. *J. Membrane Biol.* **163:**235–245
49. Sze, D.Y., Jardetzky, O. 1990. Determination of metabolite and nucleotide concentrations in proliferating lymphocytes by ^{1}H-NMR of acid extracts. *Biochim. Biophys. Acta* **1054:**181–197
50. Verkman, A.S. 2000. Water permeability measurement in living cells and complex tissues. *J. Membrane Biol.* **173:**73–87
51. Vienken, J., Zimmermann, U., Fouchard, M., Zagury, D. 1983. Electrofusion of myeloma cells on the single cell level. Fusion under sterile conditions without proteolytic enzyme treatment. *FEBS Lett.* **163:**54–56
52. Wolkers, W.F., Walker, N.J., Tablin, F., Crowe, J.H. 2001. Human platelets loaded with trehalose survive freeze-drying. *Cryobiology* **42:**79–87
53. Yancey, P. H. 1994. Compatible and counteracting solutes. *In:* Cellular and Molecular Physiology of Cell Volume Regulation. Strange, K, editor. pp 81–109, CRC, Boca Raton, FL
54. Zimmermann, H., Fuhr, G. 2003. Kryobiotechnologie: Lebende Zellen on demand. *In:* Trendbarometer Technik; Visionäre Produkte - neue Werkstoffe - Prozesse der Zukunft. Bullinger Riedel, H.-J.H. editors. pp 238–239, Hanser, München
55. Zimmermann, U., Neil, G.A. 1996. Electromanipulation of Cells. CRC Press, Boca Raton, FL